Improvement of Lift Dump on a Fighter-Type Wing at Approach Condition

Soojung Hwang*
Korea Aerospace Research Institute, Daejeon City, Korea 305-333

Ilwoo Lee**
Korea Aerospace Industries Ltd., Sacheon, Korea 664-710

Abstract

The 1/9-scale model of a fighter-type configuration was tested in the Micro-Craft 8ft x 12ft wind tunnel facility. An abrupt lift dump was found at a certain range of angle of attack under the pre-scheduled approach configuration. To avoid a probable unsatisfactory flight behavior due to the lift dump, various aerodynamic devices were suggested. Extensive tests applying the cutoff leading edge flaps, boundary layer fences, saw tooth and vortex generators were performed with flow visualization as well as force and moment measurements. Test results showed that the origin of the lift dump was caused by the secondary boundary layer flow separation generated from the strong interaction between wing and flap. Various solutions for avoiding the unfavorable feature were suggested with the merits and demerits.

Key Word : lift dump, approach configuration, boundary layer flow separation

Introduction

Korea Aerospace Industries(KAI)'s T-50 is the advanced jet trainer/lead-in fighter trainer that is being developed for the Republic of Korea Air Force and other markets. The Full Scale Development (FSD) program began in 1997. The first of four FSD aircrafts, Fig. 1, made its first flight on August 20, 2002. Four aircraft are under envelope expansion flight test, since the fourth aircraft flew first time on 4 September 2003. The supersonic T-50 has the maneuverability, endurance and advanced systems to prepare future pilots to fly next-generation fighters. These characteristics give the T-50 excellent potential as the basis for a light multi-role combat variant. Designed for high performance, the T-50 features digital fly-by-wire for precision aircraft handling, relaxed static stability to improve maneuverability, a variable camber wing with strakes to maximize the lift to drag ratio and improve directional stability, and tandem seating for superior visibility. This aircraft has an efficient turbo-fan engine utilizing proven technology for maximum reliability and safety, an advanced nav-attack sensor for multi-role missions, and an on board oxygen generating system. The T-50 is the only advanced trainer for 4th and 5th generation fighters. The aerodynamic design goals are a blend of supersonic flight, transonic maneuverability and good field performance for advanced pilot training and light combat. With extensive configuration trade studies and wind tunnel testing, the T-50 aerodynamic configuration are defined; (1) blended wing-body for subsonic minimum drag, (2) normal area distribution optimization for supersonic drag, (3) vortex lift from the strake with a variable camber wing for

* Senior Research Scientist
E-mail : soojung@kari.re.kr, TEL : 042-860-2963 FAX : 042-860-2999
** Senior Manager

Fig. 1. T-50 First Flight

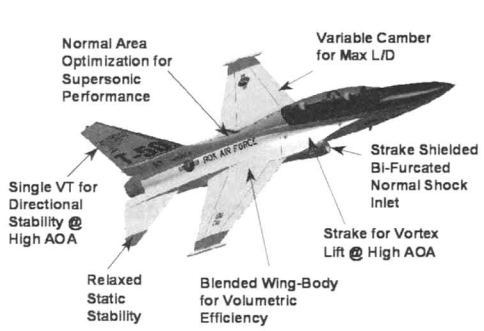

Fig. 2. T-50 Aerodynamic Features

maximum L/D during maneuvering, (4) a strake-shielded, fixed geometry normal shock inlet for good pressure recovery and stable operation throughout the flight envelope, and (5) empennage design for stability and enough control authority to prevent departure (Fig. 2). More than seven thousand hours of wind tunnel testing were performed to refine aerodynamic shap and to collect the aerodynamic database. The T-50 fly-by-wire flight control system incorporates many features that affect both airplane performance and flying qualities. One of the key elements is an automatic variable wing camber, obtained by scheduling the leading edge flap(LEF) as a function of Mach number and angle of attack(AoA). The LEF schedule provides high lift during takeoff and landing, and optimal cruise maneuvering performance in each flight phase: UA(up-and-away) configuration (gear up and flaps up) and PA(powered approach) configuration (gear and flaps down).

During low speed wind tunnel test for the PA configuration, an abrupt lift dump was observed near the power approach AoA. A Lift dump can cause unintended pitch and lateral motion, degrading the flying qualities. Several aerodynamic devices including a cutoff leading edge flap, boundary layer fences, saw tooth design and vortex generators were proposed to avoid unfavorable flying qualities during the landing approach. Flow visualization test was conducted to obtain a better understanding of the flow structure associated with the lift dump. This paper presents a description of the wind tunnel test methods and test results for the T-50 baseline configuration with and without various aerodynamic devices.

Experimental Description

Wind Tunnel Test Model and Conditions

Fig. 3 shows a $1/9^{th}$ scale full span model of the T-50 configuration installed in the Micro-Craft Low Speed Wind Tunnel. An internal balance with sting supporting system was used

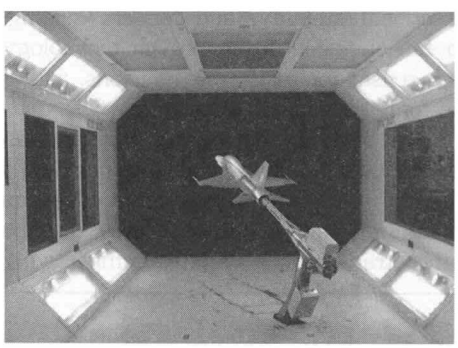

Fig. 3. T-50 Model in W/T Test Section

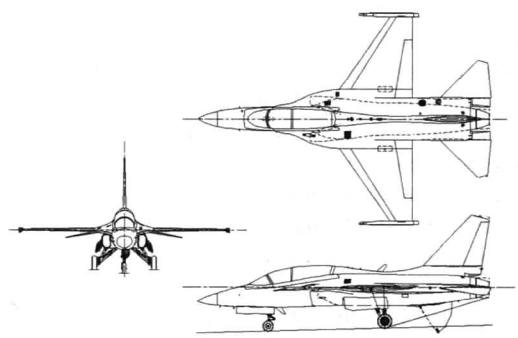

Fig. 4. T-50 Airplane Three View

for the measurement of forces and moments. Three windshields inside the nozzle of the rear fuselage were applied to estimate the internal and spillage drags. Total pressure was measured by using the eight probes of windshields, while static pressure was measured from the four probes on the surface of the sting inside the windshields. The shape of the internal duct from inlet to exhaust was designed to be well distributed to prevent the internal flow separation. But, the rear fuselage was slightly modified from the original design due to the minimum requirement of the inlet captured area ratio. The effect of the nozzle shape change on aerodynamic coefficients was corrected by computational analysis. Fig. 4 shows the T-50 aircraft three-view.

MicroCraft Low Speed Tunnel(MLST) is of conventional closed circuit design. The size of the test section is 8ft height, 12ft width and 15ft length. The test conditions can be summarized as ;

Freestream Mach Number : 0.2
Freestream Reynolds Number : 1.39 x 10^6 /ft
Freestream Dynamic Pressure : 60 psf

A transition grit was applied to the leading edge of fuselage, inlet and all the lifting surfaces in order to simulate boundary layer transition at the full scale flight condition.

Test Data Corrections

The baseline attitude of the model in this test was vertical, not horizontal. The typical test installation was wings horizontal in the MLST facility, because the horizontal attitude had lower wall correction factors and blockage effect by the remote controlled sector than vertical attitude. But the vertical installation had been used in this test to get more high angle of attack data. Fig. 5 shows lift and pitching moment curves for upright and inverted attitudes, where the upright mode means that the roll angle of the model is 90 degrees. The angularity correction was applied to AoA and pitching moment coefficient. Fig. 6 shows the measured and interpolated internal drag

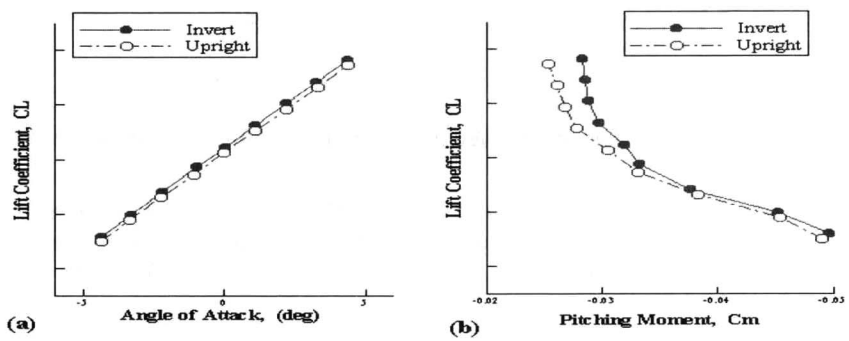

Fig. 5. Flow Angularity Effect on Lift and Pitching Moment

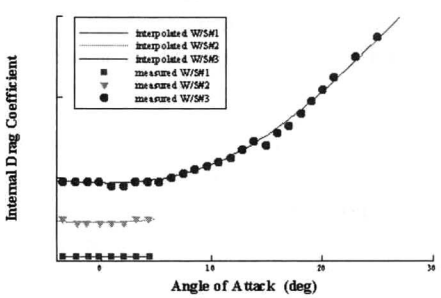

Fig. 6. Internal Drag Distributions

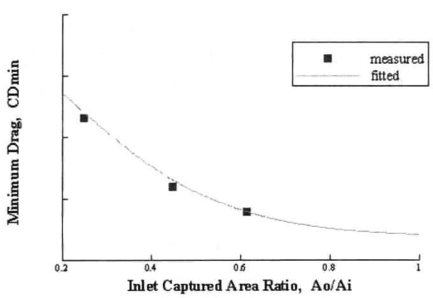

Fig. 7. Spillage Drag Distributions

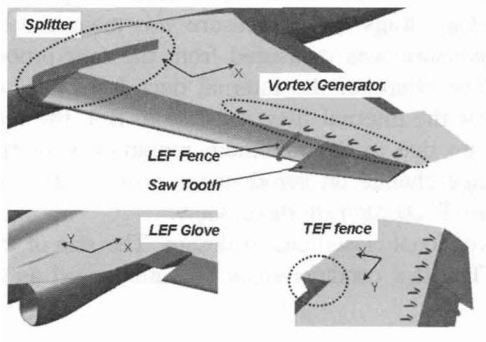

Fig. 8. Proposed Aerodynamic Devices

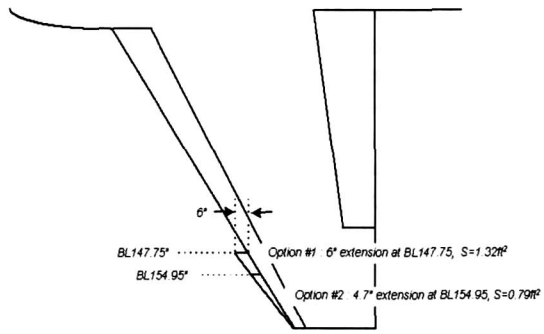

Fig. 9. Saw Teeth on Leading Edge Flap

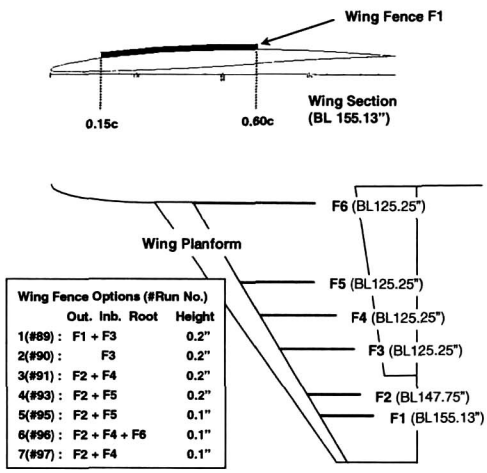

Fig. 10. Boundary Layer Fences on Wing

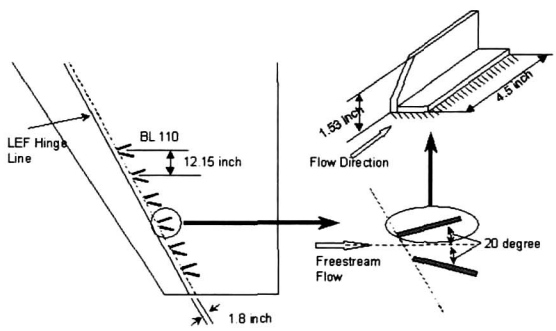

Fig. 11. Vortex Generators on Wing

distributions for the three windshields. It can be seen that the measured internal drag for AoA less than 8 degree was almost constant. The measured and interpolated spillage drag distributions on the inlet captured area ratio are shown in Fig. 7. The fitting curve from Fig. 7 was used for the correction of spillage drag.

Aerodynamic Devices

To avoid a probable unsatisfactory flight behavior due to the lift dump at approach condition, various aerodynamic devices as shown in Fig. 8 were designed and investigated in the test.

The first device is the leading edge flap cutoff. Leading edge flap was cutoff to generate the tip vortices from the side edge of remaining leading edge flap when the cutoff leading edge flap deflected. The spanwise location of the cutoff was determined as 85% of wing semispan from the flow visualization results.

The second device is saw tooth, which is often called dog tooth. The principle of saw tooth is similar to that of the cutoff leading edge flap, because the saw tooth generates tip vortices from the side edge of itself, too. The vortices wash out the boundary layer flow of lower energy on the wing, and delay the boundary layer separation. Fig. 9 shows two size options of saw tooth on the leading edge flap applied in the test.

The third device is boundary layer fence. The boundary layer fence generally plays a role of preventing the boundary layer flow moving in the spanwise direction. As a result, the boundary

layer fence can delay the secondary flow separation around the wing tip. Fig. 10 shows various options of boundary layer fence applied in the test. The fence options consist of seven total combinations with two heights and six spanwise locations as shown in Fig. 10. The height of the fence was determined by calculation of boundary layer thickness on the wing, and the spanwise locations were determined through the investigation of flow visualization results.

The fourth device is vortex generator. The vortex generator also produces tip vortices near the edge of the boundary layer, and advances the high energy flow farther into an adverse pressure gradient before separation. Fig. 11 shows the dimension and arrangement of vortex generators applied in the test.

Except for the above aerodynamic devices, the leading edge glove, the split fences, the leading and trailing edge fences as shown in Fig. 8 were applied in the test to verify their effects on the lift dump. But the detail descriptions were not discussed in this paper, because their effects were not satisfactory when compared to the other ones.

Flow Visualization

French chalk, a liquid mixture of kerosene, talc and oil, was used to visualize flow patterns on the surface of the test model. With the tunnel off line, the model was positioned to the desired test attitude and French chalk was generously applied to the model surfaces of interest. The tunnel was then run at the desired test dynamic pressure and model attitude, which was held constant. The run continued until the mixture dries, leaving a chalky white residue that traced the surface streamline patterns over regions of the model. During the run and upon completion of the run, the flow patterns were documented with photographs.

Results and Discussions

Baseline Characteristics

The T-50 uses automatic leading edge flap scheduling to get optimum aerodynamic performance in all the flight conditions. Fig. 12 shows lift, drag and pitching moment curves for

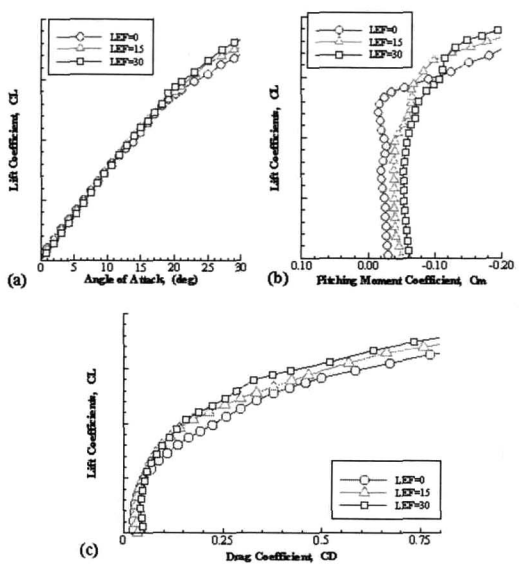

Fig. 12. Aerodynamic Characteristics at up-and-Away Condition (TEF=0°)

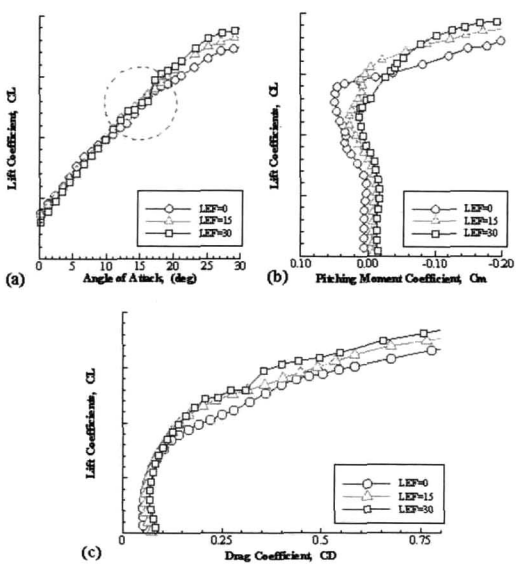

Fig. 13. Aerodynamic Characteristics at Approach Condition (TEF=20°)

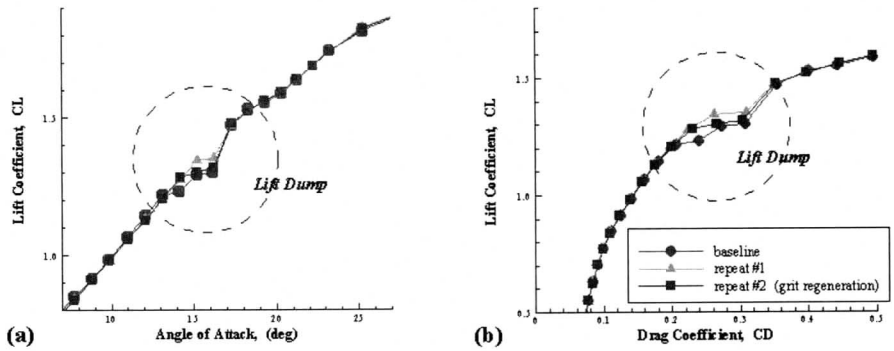

Fig 14. Lift Dump Phenomena at Approach Condition (LEF/TEF=30°/20°)

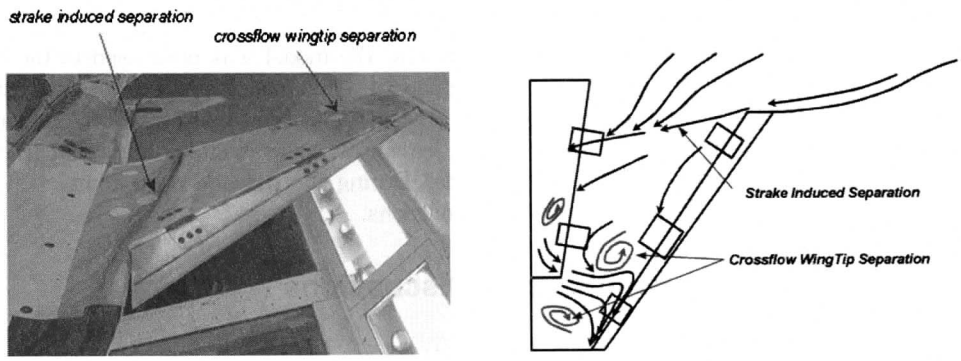

Fig. 15. Visualized Surface Streamlines (AoA=16.5°, LEF/TEF=30°/20°)

up-and-away mode with three deflection angles of leading edge flap. The trailing edge flap deflection is zero at up-and-away mode, while it is 20 degree at power approach mode. The measured minimum drag coefficient with the data correction mentioned above was 0.0236. Fig. 13 shows lift, drag and pitching moment curves for power approach mode with three deflection angles of leading edge flap.

The magnified lift curve of LEF=30° presented in Fig. 14(a) shows an abrupt lift dump with fluctuation around AoA=15°, contrary the lift curves of other cases as shown in Fig. 12(a) and Fig. 13(a). The fluctuated lift loss, which is called lift dump in this paper, can be more clearly seen from the drag polar in Fig. 13(c) and Fig. 14(b). The drag polar for LEF=30° at the approach configuration shows a big pocket around the concerned angle of attack. It can be seen from the pitching moment coefficients in Fig. 13(b) that the longitudinal stability was a little degraded by the lift dump. Fig. 14 shows lift curves measured from three repeat runs. The same phenomena can be seen around AoA=15° with a little discrepancy due to unsteadiness of the separated flow.

The lift dump was proven to be caused from the secondary boundary flow separation on the wing. Fig. 15 shows a schematic diagram with the photograph from the flow visualization by French chalk at the condition of AoA=15° and LEF/TEF =30°/20°. A strongly converged surface streamlines near the inboard wing as shown in Fig. 15 was produced by the strake induced separation. The other two separations of swirl shape on the wing were generated from the secondary boundary flow separation. The lift dump was caused from the secondary boundary layer separation near the wingtip, not the strake induced separation. The wingtip separation was asymmetric when it started to develop around the moderate angle of attack, while the strake induced separation was symmetric. From examining the visualized surface streamlines, the

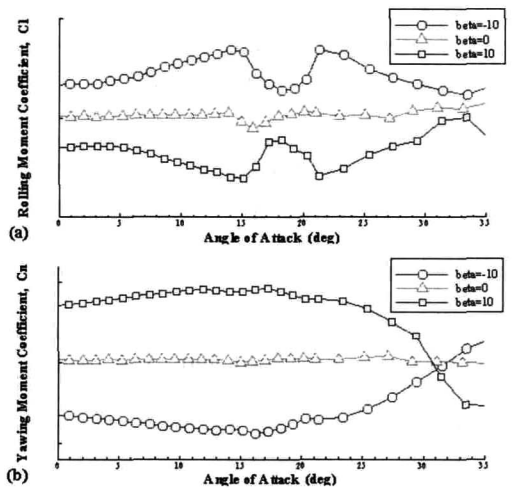

Fig 16. Lateral and Directional Characteristics at Up-and-Away Condition (LEF/TEF=30°/0°)

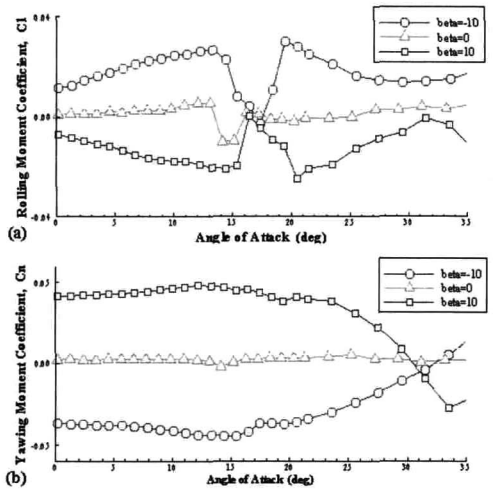

Fig. 17. Lateral and Directional Characteristics at Approach Condition (LEF/TEF=30°/20°)

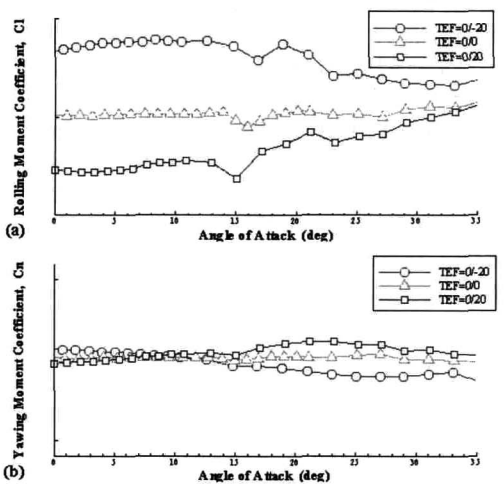

Fig. 18. Roll Control Characteristics (LEF=30°)

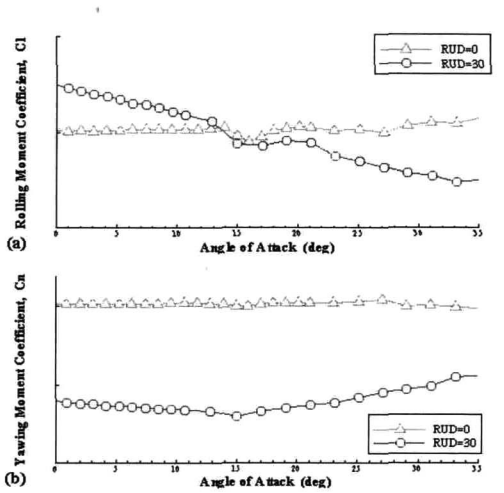

Fig. 19. Yaw Control Characteristics (LEF/TEF=30°/20°)

asymmetric boundary layer flow separation appeared at AoA=14°, and the peak of asymmetry was seen around AoA=17°. The strength of asymmetry decreased as the angle of attack went higher than 17 degrees, and finally, the symmetric separation flow was established on the left and right wings around AoA= 17°.

This history can be seen from Fig. 16 and Fig. 17 showing the yawing and rolling moments at up-and-away and approach conditions. Fig. 16 shows an abrupt drop of rolling moment coefficients, called a lateral spike in this paper, around the AoA of concerned, while the yawing moment kept continuous distribution. The lateral stability at approach condition was much more degraded as shown in Fig. 17. In the worst case, the reversal of rolling moment appeared in the specific range of the AoA of concerned. It can be seen the lateral spike from Fig. 17(a) in spite of no sideslip, while hardly seen at up-and-away condition. It should be noted that the lift dump appeared only at approach condition as shown in Fig. 14(a), while the lateral spike was found at both flight conditions as shown in Fig. 16(a) and Fig. 17(a). These kinds of lift dump and lateral

spike could produce significantly negative effects on aerodynamic performance and flying quality at the power approach flight mode. Because the concerned moderate angle of attack was the real scheduled AoA range of the approach condition to landing, and the deflection angle of LEF set from the optimum LEF schedule was 25°~30°.

On the other hand, the directional stability was little influenced from the asymmetric flow separation as can be seen from Fig. 16(b) and Fig. 17(b). It is noted that the directional stabilities were broken at an angle of attack slightly higher than approximately 30 degrees from the measured yawing moments. The comparatively high value of the stall angle of attack in directional stability was due to the vortices induced from the strake which was well designed with the blended wing and fuselage configuration.

Fig. 18 and Fig. 19 show the roll and yaw control characteristics at the condition of LEF=30°. It can be seen from Fig. 18 that the roll control power decreased with AoA, while the effect on the yawing moment increases a little. Yaw control power by rudder deflection of 30 degree as shown in Fig. 19 was almost constant as the angle of attack increased. The similar feature of asymmetry can be also seen from the test results of control power verification.

Leading Edge Flap Cutoff

Fig. 20 shows the effect of LEF cutoff on lift, drag and rolling moment characteristics at the approach condition. It was noted that the lift dump disappeared around the concerned angle of attack. It was proved that strong vortices generated from the side edge of the cutoff leading edge flap played a role of washing out the separated boundary layer flow to a certain extent. The lift curve of the cutoff LEF in Fig. 20(a) shows a clean slope, while that of the baseline shows an abrupt lift drop. The drag polars show similar characteristics, the cutoff LEF shows a very clean shape of drag polar when compared with that of the baseline LEF. Fig. 20(c) shows the effect of LEF cutoff on lateral stability. When there was no sideslip, the cutoff leading edge flap almost removed the asymmetric rolling moment around the concerned angle of attack. However, in the case of sideslip, the lateral spike still existed as shown in Fig. 20(c), but its strength was a little weakened. This means that the cutoff LEF could perfectly eliminate the lift dump, but it was not effective in sideslip condition. This can be confirmed from Fig. 21, which shows that the cutoff LEF in sideslip condition degraded lift curves around the AoA of concerned.

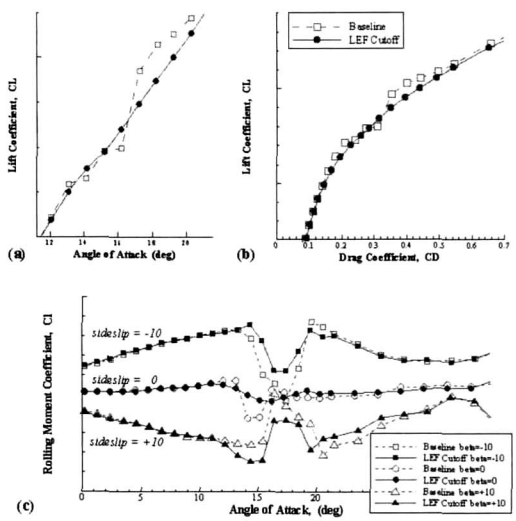

Fig. 20. Effect of Leading Edge Flap Cutoff (LEF/TEF=30°/20°)

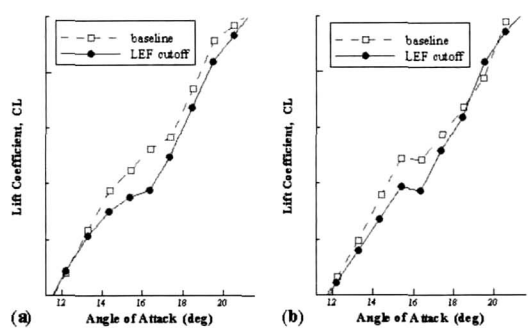

Fig. 21. Effect of Leading Edge Flap Cutoff (LEF/TEF=30°/20°, Sideslip=10°)

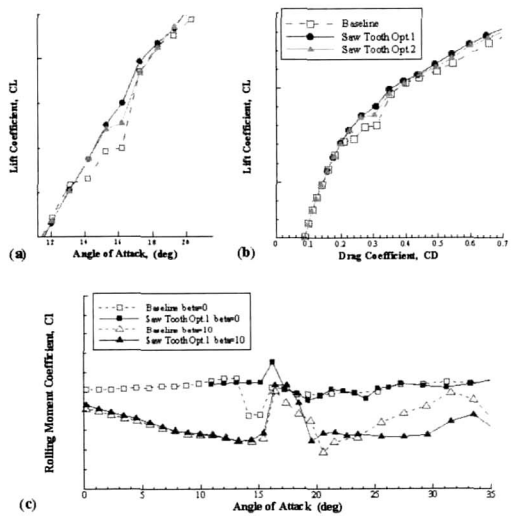

Fig. 22. Effect of Saw Teeth (LEF/TEF=30°/20°)

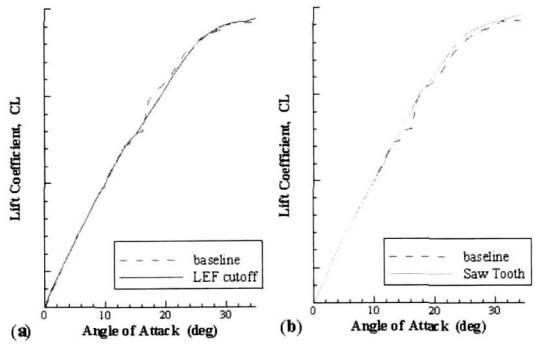

Fig. 23. Lift Curves for Cutoff LEF and Saw Tooth (LEF/TEF=30°/20°)

Leading edge flap cutoff can be an effective tool to eliminate the lift dump. One of the advantages of the LEF cutoff is that it can reduce the required hinge moment of the leading edge flap with little lift loss. This means the designer can use an actuator with relatively small capacity, eventually can get the saving of system weight. But, it should be noted that the cutoff leading edge flap may not work, or even worsen the aerodynamic characteristics in the sideslip condition as shown from Fig. 21.

Saw Tooth

Two size options of saw tooth as shown in Fig. 9 were applied to the test at approach condition. From Fig. 22 presenting the effects of saw tooth, Option 1 of bigger size gave more favorable effect on the lift bump when compared with Option 2 of smaller one. From the lift curves in Fig. 22(a), it can be said that the saw tooth was less effective on the lift dump when compared with the cutoff LEF. It was noted that the saw tooth increased the lift above the AoA of concerned, as shown in Fig. 23, contrary to the cutoff LEF. The effect of the wing area increase due to the attachment of saw tooth on lift was negligible, because no lift increase below AoA of concerned could be seen. The additional area due to the saw tooth was less than 0.5% of the total wing planform area. On the other hand, the lift increase could require higher hinge moment of leading edge flap, contrary to the cutoff LEF. The saw tooth did not show any favorable effect on lateral spikes, which can be seen from Fig. 22(c). From the test results of cutoff LEF and saw tooth, it could be concluded that vortices generated from the leading edge had a limit to remove asymmetric lateral characteristics in this test.

Boundary Layer Fence

Seven total options of boundary layer fences were applied to the wing as shown in Fig. 10. The main purpose of applying the boundary layer fences was to verify whether the lift dump originated from the secondary boundary layer flow moving in the spanwise direction. The most important factor in applying boundary layer fence was the location. Several flow visualization tests using French chalk were performed in order to determine the appropriate location of the fence. From the visualization results, the two distinguished swirl of boundary layer separation on the wing were found as shown in Fig. 15, which were proved to be induced from the secondary boundary layer flow moving in the spanwise direction. The cross flow separation around the

outboard wing showed a very strong vorticity and unsteadiness, which was proved as the origin of the lift dump. The aerodynamic blended shape of the fuselage and wing might reinforce the cross flow to the outboard wing, and make the boundary layer separation around the wingtip occur sooner. Though the location and strength of the separated vortical flows moved a little according to the angle of attack changed, the flow visualization was very helpful to understand the structure of the separated flow and to find initial locations for the fence attachment. Fig. 10 shows the location and height of the seven fence options. The length of the fences was set by 45% of local chord length.

The test results of the boundary layer fences can be summarized as followings;

(1) Option 1 : The locations of two fences were fixed at BL 155.13" and 125.25" as shown in Fig. 10, which locations were near the centers of the two lumps of boundary layer separation as shown in Fig. 15. The test result presented in Fig. 24(a) shows that it was very effective to wash out the lift dump.

(2) Option 2 : The outboard fence of Option 1 was removed in order to verify the effect of the inboard one. From the lift curve in Fig. 24(a), it can be seen that the outboard fence did not play a big role to remove the lift dump.

(3) Option 3 : The flow visualization of Fig. 15 was performed at AoA=16.5°. From the flow visualization of the other angles of attack, it was found that the separation region became wide and moved inboard as angle of attack increased. From this result, the fences of Option 1 were moved inboard as shown in Fig. 10. From the test result as shown in Fig. 24(b), Option 3 clearly washed out the lift dump around the AoA of concerned. The detail aerodynamic characteristics for Option 3 can be seen from Fig. 25. The drag polar shows a clean shape without a pocket, and the lateral characteristics were much more improved contrary to the cutoff LEF and the saw tooth. From these results, it can be said that the boundary layer fence was the most effective solution for curing this kind of asymmetric boundary layer separation in this test.

(4) Option 4 : The inboard fence of Option 3 was moved more inboard as shown in Fig. 10. The result in Fig. 24(c) shows worse effect on lift characteristics when compared with Option 3.

(5) Option 5 and 6 : The fence heights of Option 3 and 4 were reduced from 2 inch to 1 inch in order to verify the effect of the fence height on the lift dump. It can be seen from Fig. 24 that the reduction of the fence height gave a little unfavorable effect on the lift dump. It means that the height of the fence was a important factor to prevent the secondary boundary layer flow separation.

(6) Option 7 : To verify the effect of the cross flow from the upper fuselage and canopy on the lift dump, the third fence was added to Option 6 at the location of the exposed wing root as shown in Fig. 10. The test result as shown in Fig. 24(d) shows that the root fence was not effective when compared with the other ones. This means that the boundary layer cross flow moving through the wing root was not a primary source of the lift dump, and the comparatively thick blended fairing on the wing/body junction did not seriously affect the formation of lift dump.

As mentioned above, the boundary layer fence can be very effective solution to prevent the secondary flow separation at the moderate angle of attack. Boundary layer fence does not require a big design change like hinge moment increase or configuration modification. But it can give some penalty of drag rise due to the protruded configuration at high speed flight condition, as like the saw tooth.

Vortex Generator

Fig. 26 shows the effects of vortex generator on the lift dump. The dimension and arrangement of the applied vortex generators can be seen from Fig. 11. Fig. 26 shows that the lift

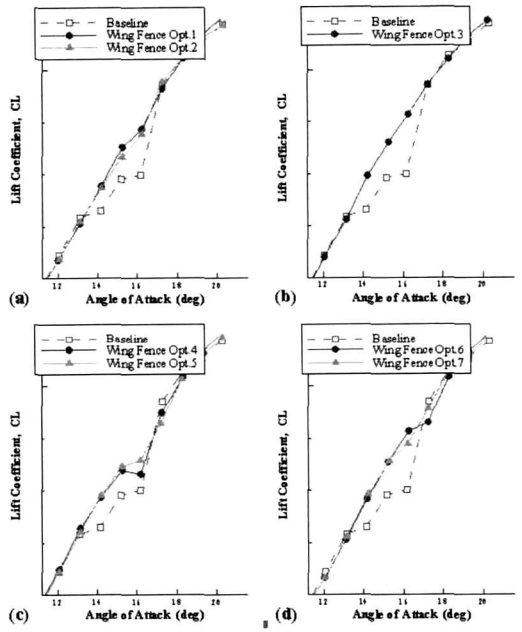

Fig. 24. Effect of Boundary Layer Fences (LEF/TEF=30°/20°)

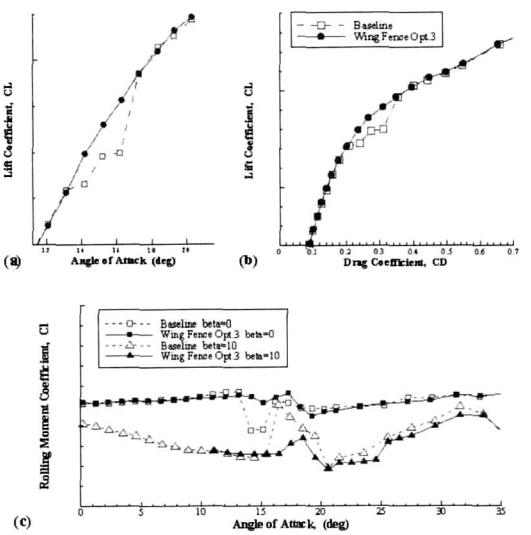

Fig. 25. Effect of Boundary Layer Fence Option.3 (LEF/TEF=30°/20°)

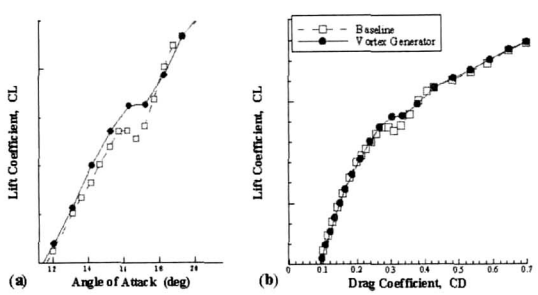

Fig. 26. Effect of Vortex Generators (LEF/TEF=30°/20°)

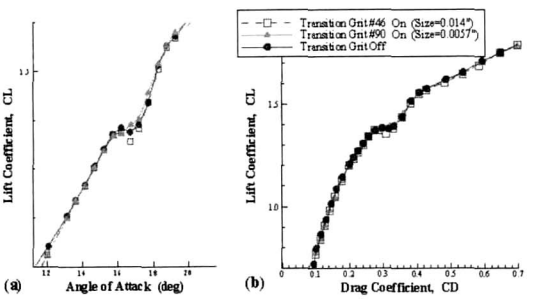

Fig. 27. Effect of Transition Grits (LEF/TEF=30°/20°)

dump was weakened by the vortex generator, but still existed. Though the other various options of vortex generator has not been tried in the test, it was concluded that the vortex generator was not a preferable solution when compared with the other ones. Because not only the result was not satisfactory, but also its application was comparatively complicated.

Real Scale Effect

The lift dump was originated from the asymmetric boundary layer flow separation at moderate angle of attack. Therefore, the characteristics of the lift dump would be dependent on local Reynolds number on the wing. It could be confirmed from Fig. 14 showing the results of several repeat runs. The data of the three test runs were measured under the same test condition, but the status of the model surface could be a little different due to the frequent configuration changes. The three lift curves in Fig. 14 shows slightly different values of lift coefficient around the concerned angle of attack, although the test data were averaged by numerous raw data gathered during enough time period at each run.

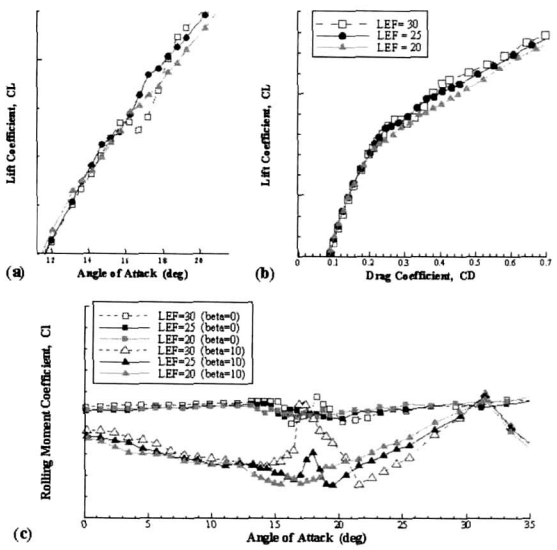

Fig. 28. Effect of LEF Deflection Angles (TEF=20°)

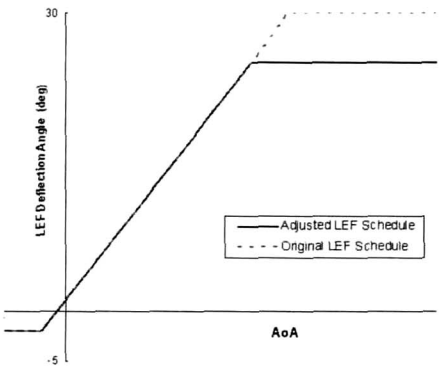

Fig. 29. LEF Schedules at Approach Condition (TEF=20°)

Fig. 27 shows the test results from three options of transition grit; (1) no grit, (2) a normal size of grit, (3) a big size of grit. Three lift curves show a little difference around the concerned angle of attack. As a result, it could be said that the lift bump was sensitive enough to be influenced by various factors like local Reynolds number, surface imperfection, transition dot and the other things to change the transition condition on the wing. If this could be applied to the real flight condition of the aircraft, the lift dump might appear in a different way with the wind tunnel test results, or even might disappear. When accepting this assumption, it could be too risky to apply the aerodynamic devices from considering only the wind tunnel test results. As a result, it was concluded that the direct application of active solutions like the aerodynamic devices was not recommended in the phase of aircraft design. If the lift bump would appear and induce a severe problem at the real scale flight condition, the boundary layer fence or the saw tooth could be a good solution for curing the unfavorable phenomena without a big design change at that time.

Leading Edge Flap Re-Scheduling

The other solution, not an aerodynamic device, for the lift dump problem is to adjust the LEF schedule. It was found that the lift dump was weakened and eventually disappeared as LEF deflection angle decreased from 30 degree in approach configuration, as shown in Fig. 28. Therefore, if the initially set optimum LEF schedule can be adjusted within acceptable boundary of performance degrade, it can be the most preferable solution for the lift dump problem. Because the re-scheduling of LEF deflection angle need not to modify the existing aircraft configuration.

Fig. 29 shows the original and adjusted LEF schedules at approach condition. But, this approach can degrade flying quality and aerodynamic performance to a certain amount, because the lift to drag ratio would decrease when compared with the case of the optimum leading edge flap schedule. Also, it should be noted that this solution is not to cure the problem contrary to the aerodynamic devices mentioned above, but just to avoid it.

Conclusions

Reviewing the low speed wind tunnel test data, two aerodynamic devices, an LEF cutoff design and a saw tooth configuration were chosen for high speed wind tunnel testing to

investigate the effects on transonic and supersonic flight. The LEF cutoff design exhibited slightly lower minimum drag with a worse drag polar, due to reduced LEF area. The saw tooth configuration increased lift as expected. But the minimum drag increased for all Mach numbers with no considerable drag polar change. An additional concern of the saw tooth configuration was increasing the hinge moment of the LEF actuator. None of the options showed significant benefits with minimum penalties and technical risks. The LEF schedule change (maximum deflection reduced to 25 deg from 30 deg) for PA configuration was selected to resolve the lift dump issue for the T-50 aircraft. No unfavorable flying qualities associated with lift dump were seen during the initial phase of T-50 flight test. Dedicated performance flight tests, a planned later phase of flight testing, will validate the lift characteristics for the PA configuration.

Acknowledgement

The authors wish to extend their sincere appreciation to all the personnel who have contributed to this paper. In particular, we gratefully acknowledge the valuable support provided by Aerodynamics Group members of T-50 Program.

References

1. H. Roh and I. Lee, "A Study of Lift Bubble Phenomena in KTX-2 Powered Approach Configuration", KSASS Conference, Seoul, Korea, April 2000.

2. Ray Whitford, "Design for Air Combat",Jane's, 1987.

3. S. Hwang and Y. Kim, "85PR0099 KTX-2 '99 #2-2P Low Speed Wind Tunnel Test Report", Korea Aerospace Ind., July, 1999.

4. I. Lee and Y. Lee, "85PR0145 KTX-2 '99 #2-2 Low Speed Wind Tunnel Test Report", Korea Aerospace Ind., August, 1999.

5. Hermann Schlichting, "Boundary Layer Theory", McGraw-Hill, 1979.

6. I. Lee and Y. Lee, "85PR0100 KTX-2 '99 High Speed Wind Tunnel Test Report", Korea Aerospace Ind., April, 1999.